Vapor Deposition of Hybrid Organic–Inorganic Dielectric Bragg Mirrors having Rapid and Reversibly Tunable Optical Reflectance

Mustafa Karaman,[†,§] Steven E. Kooi,[‡] and Karen K. Gleason*[,†,‡]

Department of Chemical Engineering and Institute for Soldier Nanotechnologies, Massachusetts Institute of Technology, Cambridge, Massachusetts 02139, and Department of Chemical Engineering, Selcuk University, Konya 42075, Turkey

Received October 30, 2007. Revised Manuscript Received January 7, 2008

Rapid (0.3 s) and reversible biomimetic response of flexible dielectric mirrors was achieved by alternating inorganic (titania) and organic (poly(2-hydroxyethyl methacrylate, pHEMA) layers. Tunable reflectance bands in the visible range resulted from water swelling of the un-cross-linked pHEMA layers, without affecting the optical thickness of the high refractive index inorganic layer, which is in precise analogy to the structural color changing mechanism employed by many natural species. Larger refractive index contrast than accessible for all organic mirrors allow the desired reflectivity to be achieved with fewer layers and hence less overall thickness. The observed optical responses quantitatively match model predictions and are completely reversible. There is no loss in reflectivity intensity upon swelling. Hybrid heterostructures were grown within a single hot-wire chemical vapor deposition (CVD) chamber, resulting in smooth and uniform nanoscale layers of high interfacial quality. To the best of our knowledge, this is the first ever combination of an inorganic thin film with a fully functional polymer thin film having interfacial smoothness at the nanoscale. The room-temperature solventless HWCVD process is scalable to large area roll-to-roll deposition and is compatible with deformable substrates such as paper and plastic.

1. Introduction

Fascinating structural coloration effects are observed in animals possessing iridophores, cells that contain stacks of thin platelets separated by gel-like cytoplasm.[1–6] Ideally, the thickness of each platelet and the cytoplasm separating them is regulated such that the reflections from each interface interfere constructively, generating a well-known one-dimensional photonic structure, a Bragg mirror. The eye of a scallop, Pecten maximus, contains 30–40 layers of high-index material guanine ($n = 1.83$) separated by low-index cytoplasm ($n = 1.33$).[3] The distinctive reflective stripes of a tropical fish Paradise whiptail are also made up of guanine-cytoplasm-based iridophores and rapid (~0.25 s) and reversible color transitions are caused by swelling and shrinking of spaces between the guanine plates, induced by osmotic movements of water in cytoplasm.[2] Natural photonic structures, such as those observed in butterfly scales, can have highly selective vapor response to individual vapors and hence potential technological applications for sensing.[7]

Thin film Bragg mirrors and other specialized thin film optical filters are manufactured commercially onto rigid substrates using inorganic materials, such as silica (SiO_2) and titania (TiO_2).[8] Typically, layer thicknesses are precisely controlled by vapor deposition, a synthesis method capable of giving high growth rates uniformity over large areas.[9] Incorporation of organic materials allows creation of deformable and tunable photonic structures.[10–12] In all organic mirrors, the refractive index contrast is low, necessitating a large numbers of layers to achieve high reflectivity.[11] Additionally, cross-linking of the adjacent polymer layers is necessary to prevent dissolution during the wet fabrication processes, which further decreases the index contrast. The resultant thick and highly cross-linked structures introduce diffusion limitations on the response time during swelling and shrinkage cycles. In a recent study,[10] the duration required for a complete shift in an all-organic Bragg structure in the reflectance band in the presence of an organic solvent was several tens of hours. Convertino and co-workers showed the possibility of tunable hybrid Bragg reflectors made from Teflon and gold as promising sensing elements.[12] The presence of metal clusters significantly improves the solvent absorbing power of the organic Teflon part, which is

* Corresponding author. E-mail: kkg@mit.edu. Tel: (617) 253-5066. Fax: (617) 258-5042.
† Department of Chemical Engineering, Massachusetts Institute of Technology.
§ Selcuk University.
‡ Institute for Soldier Nanotechnologies, Massachusetts Institute of Technology.

(1) Parker, A. R. *J. Opt. A: Pure Appl. Opt.* **2000**, *2*, R15–R28.
(2) Mathger, M. L.; Land, M. F.; Siebeck, U. E.; Marshall, N. J. *J. Exp. Biol.* **2003**, *206*, 3607.
(3) Land, M. F. *J. Exp. Biol.* **1966**, *45*, 433.
(4) Mathger, L. M.; Denton, E. J. *J. Exp. Biol.* **2001**, *204*, 2103.
(5) Ltythgoe, J. N.; Shand, J. *J. Exp. Biol.* **1989**, *141*, 313.
(6) Vukusic, P. In *Optical Interference Coatings*; Kaiser, N., Pulker, H. K., Eds.; Springer: New York, 2003; pp 1–34..
(7) Potyrailo, R. A.; Ghiradella, H.; Vertiatchikh, A.; Dovidenko, J. R.; Cournoyer, J. R.; Olson, E. *Nat. Photonics* **2007**, *1*, 123.
(8) Friz, M.; Waibel, F. In *Optical Interference Coatings*; Kaiser, N., Pulker, H. K., Eds.; Springer: New York, 2003; pp 1–34..
(9) Rancourt, J. D. *Optical Thin Films*; International Society for Optical Engineering Press, Washington, D.C., 1996; pp 24–30..
(10) Monch, W.; Denhert, J.; Prucker, O.; Ruhe, J.; Zappe, H. *Appl. Opt.* **2006**, *45, 18*, 4284.
(11) Ho, P. K. H.; Thomas, D. S.; Friend, R. H.; Tessler, N. *Science* **1991**, *285*, 233.
(12) Convertino, A.; Capobianchi, A.; Valentini, A.; Cirillo, E. N. M. *Adv. Mater.* **2003**, *15*, 1103.

10.1021/cm703107d CCC: $40.75
Published on Web 02/20/2008

normally inert and completely insoluble. The resultant hybrid structures showed much better optical performance compared to the all-organic structures. However, the time required for complete band shift was ~20 min, which is still far slower than observed in living species. Furthermore, the presence of the metal clusters renders these structures unusable in the visible range. Alternatively, tunable Bragg diffractors in the form of micro or nanoarrays of spherical particles embedded within appropriate polymer have been presented previously by many researchers. Volume change of the embedded media, or the polymer matrix, with the use of an external effect, such as solvent swelling, pH, or temperature change allowed them to be used for various sensor applications.[13–15] Asher and co-workers produced metal ion and glucose responsive sensors from crystalline colloidal array of polymer spheres polymerized within a hydrogel.[14] Using a similar swelling−shrinkage mechanism, Fudouzi and Xia demonstrated the potential of color writing using totally colorless materials.[15]

Here, we report the production of very rapid color changing hybrid materials in the form of thin film Bragg reflectors. These materials are comprised of alternating layers of the inorganic material, titania, and an organic material poly(2-hydroxyethyl methacrylate) (pHEMA). Taking advantage of the large refractive index difference between the organic and inorganic pairs, the final material is necessarily an extremely thin deformable multilayer film. Amorphous titania layers will be deposited onto room-temperature substrates and in the absence of energetic ions by employing hot-wire chemical vapor deposition (HWCVD), and thus maintaining precisely the same hardware configuration as required for deposition of swellable pHEMA. In this way, precise layering of organic and inorganic materials at nanometer scale thickness was achieved in a single deposition chamber over large areas with high uniformity. HWCVD process also allows for precise control of the layer thicknesses using real-time interferometry or quartz crystal microbalance (QCM) techniques. Titanium dioxide, when deposited as a thin film, is an excellent optical coating for dielectric mirror application due to its high transparency and refractive index.[16] The lower refractive index layer comprises pHEMA, an optically clear flexible polymer. Vapor deposited pHEMA films swell with water to form hydrogel and further lowering refractive index.[17] Many organic solvents also result in swelling of pHEMA.[18] The strong physical interaction between the hydroxyl group of polymer and Ti−O group of the inorganic matrix through hydrogen bonding prevents the swelling parallel to the substrate and confines the volume change in the swelling to one dimension, normal to the surface.[19] Hence, it is possible to tune the thickness of the low index pHEMA layer by water swelling, without affecting the optical thickness of the high refractive index inorganic layer, in precise analogy to the mechanism employed by iridophores in nature.

2. Experimental Section

2.1 Preparation of Multilayer Films. Multilayer films of PHEMA and TiO_2 were deposited on silicon, glass, quartz, polycarbonate, and paper substrates by hot-wire chemical vapor deposition in a custom built vacuum chamber.[20] In the HWCVD process, the thermal excitation of the reactant gases was achieved by resistively heating a tungsten wire array mounted next to the water circulated cooling plate on which the substrates were placed. The clearance between the filament array and the cooling plate was 35 mm. All depositions were carried out at a substrate temperature of 30 °C. For the high index layers, titanium(IV) tetra isopropoxide (TTIP) (99.999%, Aldrich) was fed to the reactor as 0.5 sccm through a temperature controlled bubbler at 50 °C, using 50 sccm O_2 (99.999%) as the carrier gas into a 20 Pa reactor pressure and a filament temperature of 600 °C. For the low index layers, the monomer 2-hydroxyethyl methacrylate (HEMA) (99.999%, Fluka) and the initiator tert-butyl peroxide (TBPO) (98%, Aldrich) were used as received. HEMA monomer was vaporized in a metal jar kept at 75 °C and fed to the reactor through a needle valve at a flow rate of 4 sccm. TBPO was kept in a glass jar and fed to the reactor through a mass flow controller at a flow rate of 4 sccm. The Poly 2-hydroxyethyl methacrylate p(HEMA) depositions were carried out at a filament temperature of 280 °C and a chamber pressure of 35 Pa. Under these conditions, the observed deposition rates were of 6 nm/min for titania and 15 nm/min for pHEMA. Hence, the deposition time for each pair in the stack was <17 min.

2.2. Film Characterizations. Real time thickness controls of the depositions were made using an interferometer equipped with a 633 nm HeNe laser source (JDS Uniphase). The ex-situ determinations of layer thicknesses and optical constants of layers were carried out using an ellipsometer (Woollam M-2000) at an angle of 70° and within a spectral range of 315−720 nm. The reflectivity measurements were carried out using a UV–vis−NIR spectrophotometer (Cary 6000i) at near normal angle. For UV–vis−NIR analysis, multilayer hybrid structures were deposited on quartz substrates, which were later placed in the instrument's gas cell accessory to allow for swelling experiments. A temperature-controlled bubbler was utilized to carry saturated water vapor into the gas cell, using nitrogen as carrier gas. The reflectivity responses of the substrates were obtained at different water vapor molar fractions in the gas cell.

Fourier transform infrared (FTIR) measurements were done on a Nicolet Nexus 870 spectrometer in normal transmission mode over the range of 400–4000 cm^{-1} at a 4 cm^{-1} resolution. X-Ray photoelectron spectroscopy (XPS) was carried out on a Cratos Axis Ultra spectrometer using a monochromatized Al Kα source.

The cross-sectional image of the hybrid Bragg structure was obtained with Transmission Electron Microscopy (TEM) (JEOL 200CX). Surface roughnesses of the deposited films were obtained from atomic force microscopy (AFM) (Digital Instruments Dimension 3000) under tapping mode using an etched standard silicon tip.

(13) Blanford, C. F.; Schroden, R. C.; Al-Daous, M.; Stein, A. *Adv. Mater.* **2001**, *13*, 26.
(14) Holtz, J. H.; Asher, S. A. *Nature* **1997**, *389*, 829.
(15) Fudouzi, H.; Xia, Y. *Adv. Mater.* **2003**, *15*, 892.
(16) Martinet, C.; Paillard, V.; Gagnaire, A.; Joseph, J. *J. Non-Cryst. Solids* **1997**, *216*, 77.
(17) Chan, K.; Gleason, K. K. *Langmuir* **2005**, *21, 19,]?>*, 8930.
(18) Goustouridis, D.; Chatzandroulis, S.; Raptis, I.; Valamontes, E. S. In *Proceedings of IEEE Sensors 2004*, Third International Conference on Sensors, Vienna, Austria, Oct 24−27, 2004; IEEE: Piscataway, NJ, 2004; Vol. 1, p 162.
(19) Hu, Q.; Marand, E. *Polymer* **1998**, *40*, 4833.
(20) Gupta, M.; Gleason, K. K. *Thin Solid Films* **2006**, *515*, 1579.

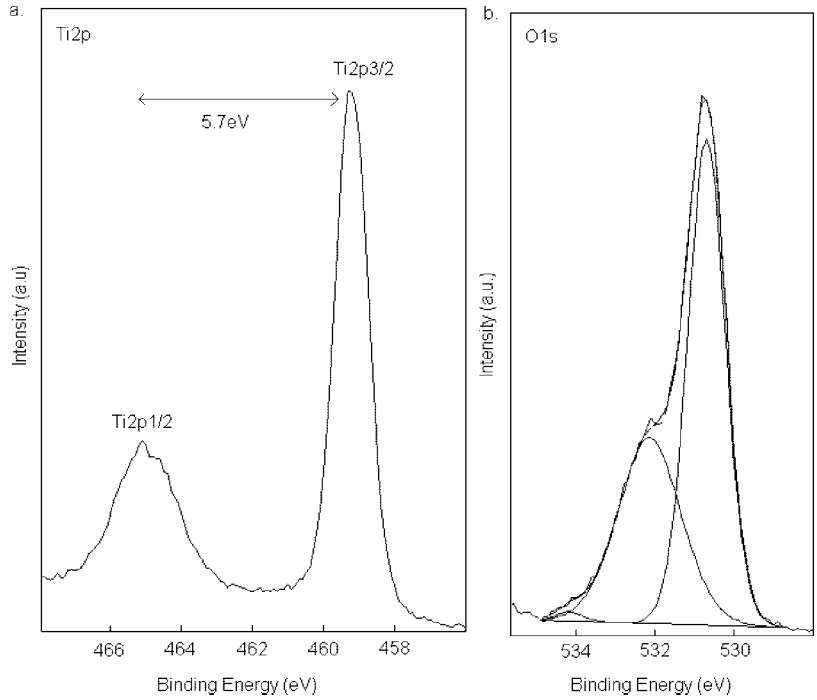

Figure 1. Ti_{2p} and 0_{1s} high-resolution XPS scans of the titania film deposited from HFCVD.

3. Results and Discussion

Thicknesses and optical constants of individual TiO_2 and pHEMA layers deposited on silicon substrates were determined by using spectroscopic ellipsometry at an incident angle of 70°. Refractive indices of the titania and pHEMA layers at $\lambda = 500$ nm were determined to be 1.81 and 1.51, respectively, with negligible extinction coefficients. The refractive index of the titania layer is lower than that of amorphous TiO_2 (∼2) and can be attributed to carbon incorporation from titanium tetra isopropoxide (TTIP) precursor, as is commonly observed in metal oxide deposition at low substrate temperature.[21] XPS analysis indicates an O/Ti atomic ratio between 2 and 3, with a carbon content of ∼20%. In Figure 1a, the high-resolution XPS spectrum shows intense peaks for $Ti_{2p3/2}$ and $Ti_{2p1/2}$ centered at the binding energy values of 459.2 and 464.9 eV correspond, respectively, to the identical binding energies observed for stoichiometric TiO_2.[21] The nonlinear least-squares fit of the O_{1s} state (Figure 1b) indicates a major component centered at a binding energy value of 530.8 eV, which indicates Ti−O bond. The shoulder on the left-hand side of Figure 1b centered at 532.3 eV corresponds to the hydroxyl species, which are most probably incorporated from the H_2O, which is formed in the CVD chamber as a reaction byproduct. While TiO_2 layers can often quite rough,[22,23] Atomic force microscopy (AFM) reveals that the HWCVD titania layers are extremely smooth (rms roughness ∼0.8 nm) (Figure 2), most likely indicating an amorphous nature as a result of the carbon moieties. The refractive index of pHEMA layers

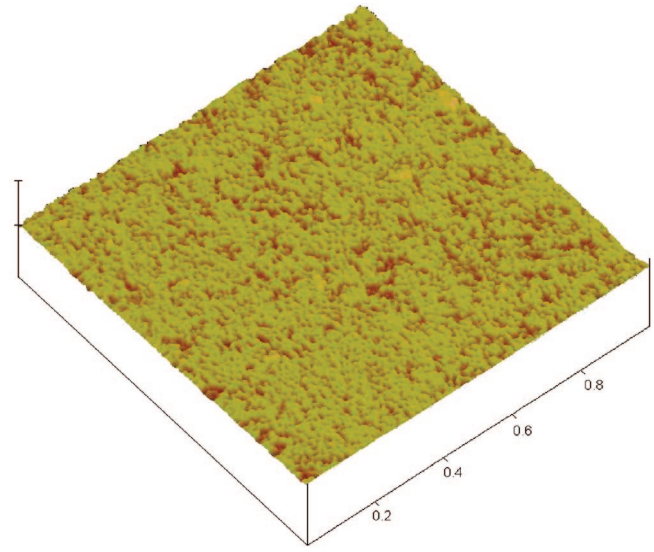

Figure 2. Atomic force micrograph of the HFCVD titania film deposited on Si wafer.

is the same as previously reported values.[17] As was also previously observed,[17] the FTIR spectrum of the iCVD PHEMA film deposited on a silicon substrate (Figure 3) shows strong absorption peaks for O−H stretching (3700–3050 cm^{-1}), C−H stretching (3050–2700 cm^{-1}), *C*═O stretching (1750–1690 cm^{-1}), C−H bending (1500–1350 cm^{-1}), and C−O stretching (1300–1200 cm^{-1}) and O−H stretching. The broad peak centered at 3450 cm^{-1} and the strong peak centered at 1730 cm^{-1} indicate the retention of the hydroxyl and carbonyl groups, respectively. Hence, the FTIR analysis indicates the retention of the entire pendant hydroxyethyl ($-CH_2CH_2OH$) functionality, which is responsible for the hydrophilic nature of the films and allows for the polymer to swell in water extensively. The large refractive index difference between the organic and inorganic layers allows

(21) Babelon, P.; Dequiedt, A. S.; Mostefa-Sba, H.; Bourgeois, S.; Sibillot, P.; Sacilotti, M. *Thin Solid Films* **1998**, *322*, 63.
(22) Bernardi, M. I. B.; Lee, E. J. H.; Lisboa-Filho, P. N.; Leite, E. R.; Longo, E.; Varela, J. A. *Mater. Res.* **2001**, *4*, 223.
(23) Huang, H.; Yao, X. *Surf. Coat. Technol.* **2005**, *191*, 54.

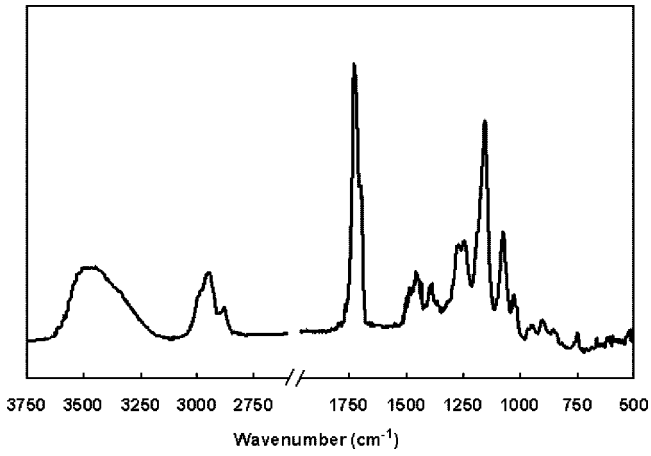

Figure 3. FTIR absorbance spectrum of PHEMA film deposited from HFCVD.

Figure 4. TEM image of a 9-layer stack of titania-pHEMA deposited on (100) p-type silicon wafer. Dark layers are titania and white layers are pHEMA.

high reflectivity values with low number of pairs; hence the resultant highly reflective structures can be extremely thin. The cross-sectional image of the hybrid Bragg structure (Figure 4) was obtained with transmission electron microscopy (TEM) (JEOL 200CX) and clearly resolves the precise layering of 9 successive organic–inorganic layers within just 300 nm thick film. The high-density titania regions are much darker than the low density polymer layers. Such a high quality layering of organic and inorganic thin films in a multilayer stack of a few hundreds of nanometers thickness was not observed clearly in previous studies. The sharp interface between the organic and inorganic phases and highly reproducible layer thickness accounts for the high performance of these multilayer structures as optical dielectric coatings.

The ability to produce the hybrid multilayer structures at room temperature and in a solvent-free, dry atmosphere allowed many different types of substrates to be coated (Figure 5): microscope glass, quartz, polymer (polycarbonate, poly vinyl chloride and PDMS sheets) and paper substrates. The mechanical integrity of the multilayer stack on the flexible substrates is evidenced by the lack of change on the visual appearance or on the structural integrity of the structures even after hundreds of deformation events.

A seven layer hybrid structure of (titania−pHEMA)^3−titania multilayer film was deposited on a quartz disk (Figure 5b), which was subsequently mounted as the window of a gas cell of a UV–visible spectrophotometer (Figure 7). The experimental reflectance spectra of the Bragg structure (Figure 6a) are plotted as a function of wavelength, together with the theoretical reflectance spectra (black lines). In order to find the overall theoretical reflectivity of the multilayer film, the transfer matrix method was utilized.[24] For each layer in the structure, a 2×2 matrix was defined using the layer thickness and refractive index. Overall theoretical responses were obtained by multiplying all of the matrices contributing to the structure in the order they appear in the structure. Curve I in Figure 6a shows the reflectivity of an as-deposited dry stack in which the layer thickness of 64 nm for the titania and 77 nm for pHEMA both correspond to $\lambda/4 = 115$ nm. As expected, the observed maximum intensity of reflection occurs at 460 nm. Upon exposure to the saturated water vapor, the reflectivity band shifted in <1 s to the longer wavelengths (490 nm). Curve II in Figure 6a shows a band shift of 30 nm caused by 6.7 mol % water vapor in nitrogen. The shift in the reflectivity band increased up to 70 nm at 10 mol % of water vapor (curve III). Decreasing the water percentage back to 6.7 mol %, the reflectivity band returned to curve II (see dashed line), and when the water vapor exposure ceased, all spectra returned to the original position (curve I, dashed line), indicating reversible performance. Almost the same optical responses were observed after many swelling−shrinkage cycles, which indicates that the structural integrity of the films was preserved even after the repeated exposure to the solvent vapors. Another important outcome of Figure 6a is that the shapes of the reflectance peaks in each case do not change with swelling-shrinkage cycles. This implies equivalent swelling of each individual polymer layer in the stack. If differences in behavior had existed between the polymer layers, asymmetric reflectance peaks would be observed upon swelling of the stack. Another advantage of the hybrid Bragg structure is that there is not any intensity loss upon swelling (Figure 6a). One may expect that there should be some loss in intensity of the reflectance band upon swelling, because of the disruption of the quarter wave periodicity. However, that loss in intensity is balanced with a decrease in the refractive index of the low index polymer layer.

The response of the Bragg reflector in the presence of water vapor is very quick. Figure 7 shows the photographs of the coated swelling cell window during a color tuning cycle in the presence of solvent vapor. The quartz cell window contains a 7 layer (titania−pHEMA)^3−titania hybrid structure, designed to reflect greenish light with $\lambda/4 = 140$ nm. The change from green to red phase is accomplished within approximately 0.3 s. The complete reversal back to the green state also occurs in approximately 0.3 s. Overall swelling cycle occurs in less than a second. The extremely short cycle times result from combining the very thin nature of the hybrid stack together with the linear structure of the acrylic polymer layer,

(24) Born, M.; Wolf, E. *Principles of Optics*, 6th ed.; Cambridge University Press: Oxford, U.K., 1980; Vol. 5, pp 1–70..

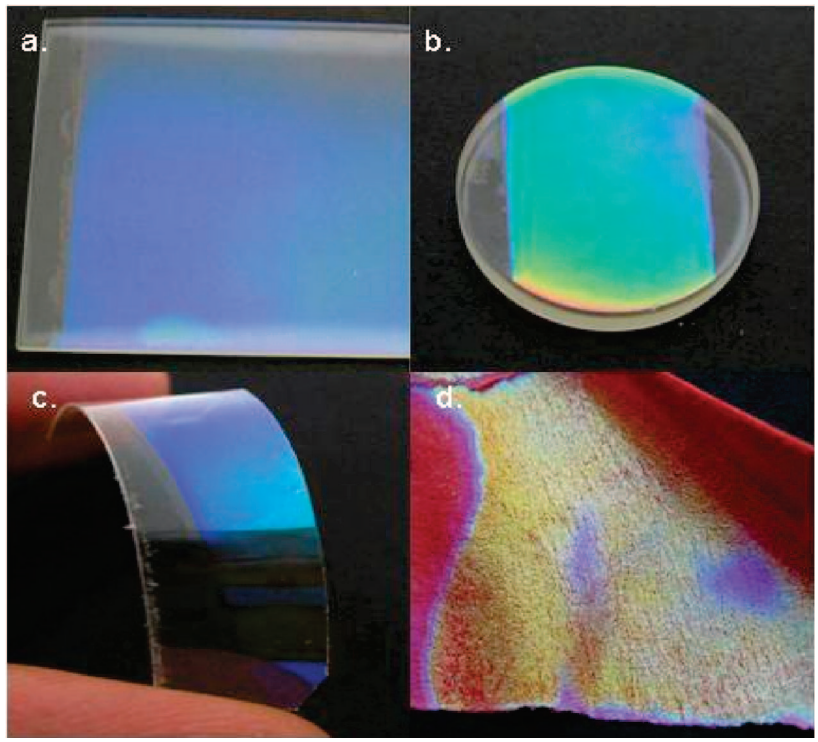

Figure 5. Hybrid Bragg structures deposited on various substrates: (a) microscope glass (2.5 × 5 cm), (b) quartz (2 cm in diameter), (c) polycarbonate (2 × 5 cm), and (d) red paper (1.5 × 3 cm).

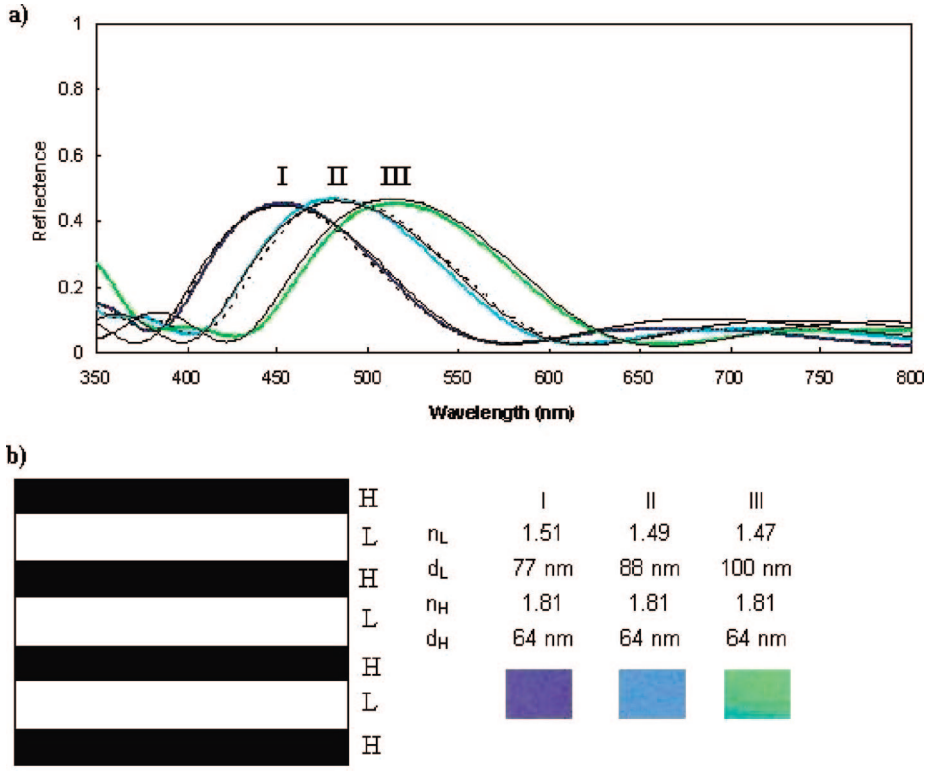

Figure 6. (a) Experimental and theoretical reflectivity responses of a seven-layer titania (H)−pHEMA (L) hybrid structure in dry (I) and swollen phases (II and III, corresponding to 6.7 and 10 mol % water vapor, respectively; dashed lines near curve I and curve II correspond to the reversed states); (b) the schematic multilayer structure with designed optical parameters (I), and experimentally observed optical parameters after swelling (*n* represents refractive index and *d* represents thickness; the colored boxes under columns I, II, and III are the actual images cropped from the quartz window photographs taken during dry and swollen states, respectively).

which maintains full retention of the hydrophilic chemical functionality. Both the overall thinness and lack of cross-linking in the organic layer promote rapid solvent diffusion in comparison to previously reported thicker stacks comprised of cross-linked polymer layers.[10] Such short response times are typical for the Bragg structures observed in natural species, such as scales of paradise whiptail, for which the phase transition from blue resting

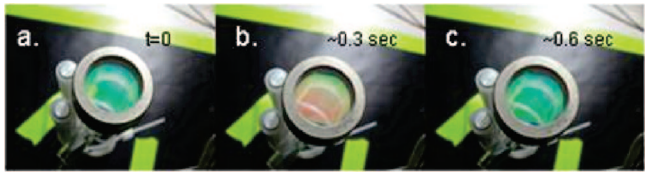

Figure 7. Photographs of the color change of the coated window (Figure 5b) in the swelling cell with corresponding occurrence times: (a) green phase (dry, as-deposited), (b) red phase caused by 1 mol% water vapor in N_2, (c) recovered green phase (after N_2 purging).

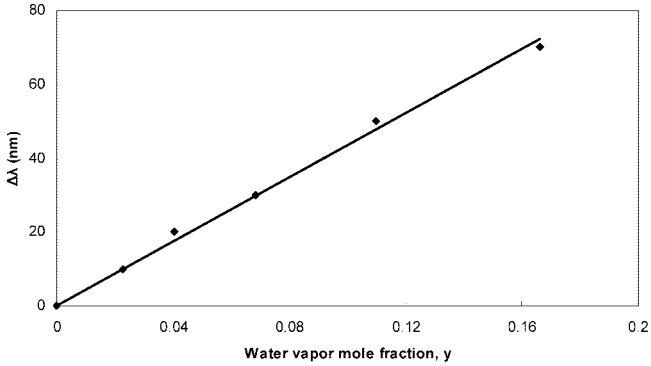

Figure 8. Shift in the position of high reflectivity peak versus water vapor mole fraction ($\lambda_o = 460$ nm for the dry film, $\Delta\lambda$ is the difference between the wavelength of the high reflectivity peak after and before exposure to the water vapor).

phase to the red phase occurs within around 0.25 s^2. In addition to the response speed, the response sensitivity is another important measure to evaluate sensing performance of the Bragg structures for any sensor application. The sensitivity of the hybrid Bragg structure is illustrated in Figure 8, where the shift in the position of the high reflectivity peak before and after exposure to the water vapor at different mole fractions are presented. A linear dependence of the absorptance peak shift on the water vapor concentration in nitrogen was observed, and a sensitivity value of 0.42 pm/ppm was estimated in the visible portion of the electromagnetic spectrum for the studied composition range.

4. Conclusions

It is shown that precise layering of hybrid organic and inorganic multilayer thin films can be produced at nanometer scale in a single-stage vapor deposition method. The HWCVD approach is capable of producing smooth and uniform surfaces within very short production times over large areas without any heat, radiation, or solvent damage on the substrate, which gives freedom to select almost any type of substrates including papers, plastics, glasses, etc. Very fast and reversible biomimetic response of hybrid multilayers with tunable reflectance bands proved the superior optical performance of the structures. The flexibility and durability of the films may allow them to serve in many different areas including organic vapor detection systems. Easy and precise control of the layer thicknesses will allow the production of more advanced filter designs on various substrates.

Acknowledgment. This research was supported by, or supported in part by, the Defense Advanced Research Projects Agency and the U.S. Army through the Institute for Soldier Nanotechnologies, under Contract DAAD-19-02-0002 with the U.S. Army Research Office. The work also made use of the MRSEC Shared Facilities supported by NSF Grant DMR-9400334. M.K. was financially supported in part by the Scientific and Technological Research Council of Turkey (TUBITAK).

CM703107D